

A solvable 3D Kondo lattice exhibiting pair density wave, odd-frequency pairing and order fractionalization

Piers Coleman,^{1,2} Aaditya Panigrahi,¹ and Alexei Tsvelik³

¹Center for Materials Theory, Department of Physics and Astronomy,
Rutgers University, 136 Frelinghuysen Rd., Piscataway, NJ 08854-8019, USA

²Department of Physics, Royal Holloway, University of London, Egham, Surrey TW20 0EX, UK.

³Division of Condensed Matter Physics and Materials Science,
Brookhaven National Laboratory, Upton, NY 11973-5000, USA

(Dated: July 21, 2022)

The Kondo lattice model plays a key role in our understanding of quantum materials, but a lack of small parameters has posed a long-standing problem. We present a 3 dimensional $S = 1/2$ Kondo lattice model describing a spin liquid within an electron sea. Strong correlations in the spin liquid are treated exactly, enabling a controlled analytical approach. Like a Peierls or BCS phase, a logarithmically divergent susceptibility leads to an instability into a new phase at arbitrarily small Kondo coupling. Our solution captures a plethora of emergent phenomena, including odd-frequency pairing, pair density wave formation and order fractionalization. The ground-state state is a pair density wave with a fractionalized charge e , $S = 1/2$ order parameter, formed between electrons and Majorana fermions.

The rich physics of the Kondo lattice, describing an array of local moments interacting with an electron sea, plays a key role in our understanding of quantum materials, from heavy fermion compounds to twisted moiré lattices [1–4]. A key element of this model is the fractionalization of spins into heavy fermions, producing a large Fermi surface. These interactions have to date been treated with approximate methods, such as the large- N expansion[5–9] and dynamical mean field theory[10].

Our work builds on a series of important developments in the theory of Kitaev models and their connection with the Kondo lattice[11–16]. Earlier variants of Kitaev-Kondo lattices include models that couple the original, spin-gapped Kitaev spin liquid to a conduction sea [13–15], and models that couple two dimensional Yao-Lee spin liquid to a conduction sea via an octupolar coupling[16].

Here we introduce a 3-dimensional Kondo lattice model which couples a Z_2 spin liquid with a Fermi surface to a conduction sea, in which the Kondo lattice physics can be treated analytically to leading logarithmic accuracy. The spin fluid is a three dimensional generalization of the Yao Lee spin liquid[17], embedded on a hyper-octagonal lattice[11], chosen because its cubic, trivalent structure gives rise to an exactly solvable, gapless spin liquid whose gapless Majorana excitations lie on a Fermi surface. Like the Kitaev spin liquid, the Z_2 gauge fields associated with the fractionalized spins are static and can be treated exactly [17, 18].

Recent work has hypothesized that hybridization between electrons and fractionalized excitations can give rise to a new kind of *fractionalized order* with half-integer quantum numbers[19, 20]. Our Kondo lattice model provides a rigorous example of this phenomenon. In particular, at half filling, the judicious choice of the lattice guarantees a perfect nesting between spinon and electron Fermi surfaces and allows us to sum the leading logarithmic divergences, establishing an instability at infinitesimal Kondo coupling into a pair-density wave with a charge e , $S = 1/2$ order parameter, which induces

odd-frequency pairing amongst the conduction electrons and also gives rise to a neutral, Majorana Fermi surface.

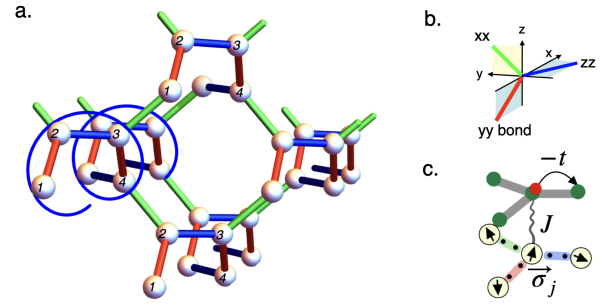


FIG. 1. (a) Hyper-octagonal lattice: a four-atom coil (1, 2, 3, 4) on a BCC lattice gives rise to alternating square and octagonal spirals[11].(b) Anisotropic coupling of orbital degrees of freedom according to the plane in which the bond lies. (c) Kondo coupling between the Yao-Lee spin liquid and the electron sea.

Our model Hamiltonian $H = H_C + H_{YL} + H_K$, where

$$\begin{aligned}
 H_C &= -t \sum_{\langle ij \rangle} (c_{i\sigma}^\dagger c_{j\sigma} + \text{H.c.}) - \mu \sum_j c_{j\sigma}^\dagger c_{j\sigma}, \\
 H_{YL} &= (K/2) \sum_{\langle ij \rangle} (\vec{\sigma}_i \cdot \vec{\sigma}_j) \lambda_i^{\alpha_{ij}} \lambda_j^{\alpha_{ij}}, \\
 H_K &= J \sum_j \vec{S}_j \cdot (c_j^\dagger \vec{\sigma} c_j).
 \end{aligned} \tag{1}$$

Here $\langle i, j \rangle$ are neighboring sites on the hyper-octagonal lattice[11], a trivalent body centered cubic (BCC) crystal with four atoms per primitive unit cell, coiled around a helix to form alternating square and octagonal spirals(Fig. 1). H_C describes hopping electrons while H_{YL} describes a three-dimensional Yao-Lee (3DYL) spin liquid on the same lattice, with an orbital and spin degree of freedom at each site, denoted by Pauli operators λ_j^a ($a = 1, 2, 3$) and spins $\vec{S}_j = \vec{\sigma}_j/2$, respectively. The $\alpha_{ij} = x, y, z$ label anisotropic xx, yy and zz orbital interac-

tions on bonds that lie in the yz , zx and xy planes respectively. Finally, J is an antiferromagnetic Kondo coupling between the electrons and local moments.

Fermionization. The Yao-Lee model [17] belongs to a family of Z_2 Kitaev spin liquids which can be solved exactly using fermionization. Following [17] we represent spin and orbital operators as products of Majorana fermions $\vec{\sigma}_j = -i\vec{\chi}_j \times \vec{\lambda}_j$ and $\vec{\lambda}_j = -i\vec{b}_j \times \vec{b}_j$, where we use the normalization $\{\chi_i^a, \chi_j^b\} = \delta_{ij}\delta^{ab}$. The spin-orbital operator is given by $\vec{\sigma}_j \lambda_j^\alpha = -2iD_j \vec{\chi}_j b_j^\alpha$ where the constants $D_j = 8i\chi_j^1 \chi_j^2 \chi_j^3 b_j^1 b_j^2 b_j^3 = \pm 1$ commute with H . In the gauge $D_j = 1$,

$$H_{YL} = K \sum_{\langle i,j \rangle} u_{ij} (i\vec{\chi}_i \cdot \vec{\chi}_j) \quad (2)$$

where $u_{ij} = -2ib_i^{\alpha ij} b_j^{\alpha ij} = \pm 1$ is a Z_2 gauge field that commutes with the Hamiltonian.

The 3DYL model describes free fermions moving in a static Z_2 gauge field. This model shares many of the properties of a 2D Kitaev spin liquid, most notably, the presence of gapped Z_2 flux excitations. On the hyper-octagonal lattice these are described by Wilson loops - products of the gauge fields $W = \prod u_{(i,j)} = \pm 1$ around closed ten and twelve-fold loops (where (i,j) orders the sites i and j along xx , yy and zz bonds so that the site furthest in the y , z and x directions respectively, is placed first [11]). In the spin liquid ground-state, all loops are trivial $W = 1$ [11]; flipping the sign of a Wilson loop creates a flux excitation (vison), with an energy determined as a fraction of K . Unlike 2D Kitaev spin liquids, the 3 dimensional models undergo an Ising phase transition into a Higgs phase where gauge fluctuations are suppressed and Wilson loops develop long-range order [21–23]. For the Kitaev model on the hyper-octagon lattice the transition at $T_{c1} \sim 0.012K$ [22, 23] gives rise to a spin-gap, but in the 3DYL, spin excitations occur without the creation of visons, eliminating the spin-gap; moreover, the three Majorana modes enhance T_{c1} by a factor of three. Below T_{c1} gauge fluctuations are suppressed and the Majorana fields describe coherent, fractionalized spin excitations.

In the ground-state, choosing a gauge where $u_{(i,j)} = 1$ and taking into account that $\chi_{-\mathbf{k}} = \chi_{\mathbf{k}}^\dagger$,

$$H_{YL} = K \sum_{\mathbf{k} \in \square} \vec{\chi}_{\mathbf{k}\alpha}^\dagger h(\mathbf{k})_{\alpha\beta} \vec{\chi}_{\mathbf{k}\beta}, \quad (3)$$

where $\alpha, \beta \in [1, 4]$ are site indices, while

$$h(\mathbf{k}) = \begin{pmatrix} 0 & i & ie^{-i\mathbf{k}\cdot\mathbf{a}_2} & ie^{-i\mathbf{k}\cdot\mathbf{a}_1} \\ -i & 0 & -i & ie^{-i\mathbf{k}\cdot\mathbf{a}_3} \\ -ie^{i\mathbf{k}\cdot\mathbf{a}_2} & i & 0 & -i \\ -ie^{i\mathbf{k}\cdot\mathbf{a}_1} & -ie^{i\mathbf{k}\cdot\mathbf{a}_3} & i & 0 \end{pmatrix}, \quad (4)$$

and $\mathbf{a}_1 = (1, 0, 0)$; $\mathbf{a}_2 = \frac{1}{2}(1, 1, -1)$; $\mathbf{a}_3 = \frac{1}{2}(1, 1, 1)$, are the primitive BCC lattice vectors. Since $\chi_{-\mathbf{k}} = \chi_{\mathbf{k}}^\dagger$, the momentum sum is restricted to half the Brillouin zone, corresponding to a

cube (\square) of side length 2π centered at the P point at (π, π, π) . The spectrum $E_{\mathbf{k}} \equiv K\epsilon(\mathbf{k})$, determined by $\det[\epsilon\mathbf{1} - h(\mathbf{k})] = 0$, or

$$\epsilon^4 - 6\epsilon^2 - 8\epsilon(s_x s_y s_z) + [9 - 4(s_x^2 + s_y^2 + s_z^2)] = 0, \quad (5)$$

(where $s_l \equiv \sin(k_l/2)$, $l = x, y, z$), contains a *single* Fermi surface centered at P [12] (Fig. 2).

Since the electrons and majoranas move on the same lattice, at half filling their Fermi surfaces are perfectly nested and can be brought into coincidence by applying a gauge transformation to the electrons,

$$(c_1, c_2, c_3, c_4)_{\vec{R}} \rightarrow e^{-i\mathbf{Q}\cdot\mathbf{R}}(c_1, ic_2, c_3, -ic_4)_{\vec{R}}, \quad (6)$$

where $\mathbf{Q} = (\pi, \pi, \pi)$ and $\mathbf{R} = n_1\mathbf{a}_1 + n_2\mathbf{a}_2 + n_3\mathbf{a}_3$ locates the unit cell. In this gauge,

$$H_c = \sum_{\mathbf{k} \in BZ} c_{\mathbf{k}\sigma\alpha}^\dagger [-t h(\mathbf{k}) - \mu\mathbf{1}]_{\alpha\beta} c_{\mathbf{k}\sigma\beta}, \quad (7)$$

and H_{YL} (3) have the same form. At low temperatures, where flux excitations can be ignored, we can rewrite the Kondo interaction in terms of the spin $\vec{S}_j = -(i/2)\vec{\chi}_j \times \vec{\chi}_j$ and decouple it using a Hubbard-Stratonovich transformation, in terms of a charge e spinor, $V_j = (V_{j\uparrow}, V_{j\downarrow})^T$,

$$H_K = \sum_j \left[(c_j^\dagger \vec{\sigma} V_j) \cdot \vec{\chi}_j + \text{H.c.} \right] + 2 \frac{V_j^\dagger V_j}{J} \quad (8)$$

The terms multiplying $\vec{\chi}_j$ must themselves be Majorana fermions, enabling us to rewrite H_K in the compact form

$$H_K = \sum_j \left[-iV_j(\vec{c}_j \cdot \vec{\chi}_j) + \frac{V_j^2}{J} \right], \quad (9)$$

where we have cast $V_j = (V_j/\sqrt{2})(z_{j\uparrow}, z_{j\downarrow})^T$ in terms of a normalized spinor and a real amplitude $V_j/\sqrt{2}$, dividing the electrons into four Majorana components, (c_j^0, \vec{c}_j) ,

$$\begin{pmatrix} c_{j\uparrow} \\ c_{j\downarrow} \end{pmatrix} = \frac{1}{\sqrt{2}}(c_j^0 + i\vec{c}_j \cdot \vec{\sigma}) \begin{pmatrix} z_{j\uparrow} \\ z_{j\downarrow} \end{pmatrix}. \quad (10)$$

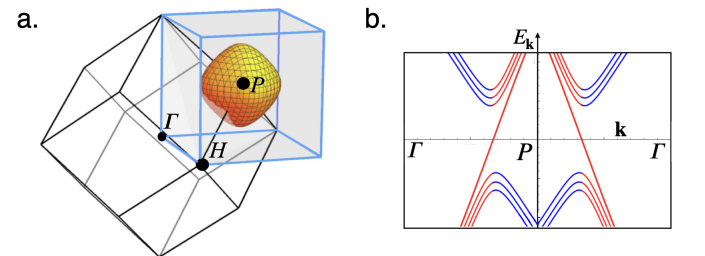


FIG. 2. (a) Majorana Brillouin zone of the hyper-octagonal lattice showing coincident conduction and Majorana Fermi surfaces around the P point. (b) Hybridization of Majorana modes (in blue) with conduction band (in red) leaves one conduction Majorana band decoupled, forming a neutral Majorana surface.

Thus in a coherent Kondo lattice, the vector components of the electron hybridize with the spinons and the scalar component decouples.

Now the field V_j is a fluctuating field inside the path integral, but the nesting between the Majorana and conduction Fermi surfaces ensures that it has a susceptibility to condense that is logarithmically divergent in temperature or chemical potential. Like a Cooper or Peierls instability, this ensures that instability into a condensed phase must occur for arbitrarily weak Kondo coupling.

We shall now focus on the stable, uniform condensate $V_j = V$. At half-filling ($\mu = 0$), vector and scalar electron components decouple, so that

$$H = \sum_{\mathbf{k} \in \square} \left[-t c_{\mathbf{k}}^{0\dagger} h_{\mathbf{k}} c_{\mathbf{k}}^0 + \vec{\psi}_{\mathbf{k}}^\dagger \begin{pmatrix} -t h_{\mathbf{k}} & -iV \\ iV & K \hat{h}_{\mathbf{k}} \end{pmatrix} \vec{\psi}_{\mathbf{k}} \right] + \frac{NV^2}{J}, \quad (11)$$

where $\vec{\psi}_{\mathbf{k}} = (\vec{c}_{\mathbf{k}}, \vec{\chi}_{\mathbf{k}})^T$, N is the number of sites and we denote $h_{\mathbf{k}} \equiv h(\mathbf{k})$.

As we now demonstrate, at a temperature T_{c2} , below the Ising phase transition T_{c1} , the system undergoes a second phase transition where the spinor order parameter V condenses (Fig. 3a). To demonstrate the instability, we note that since only states close to the Fermi surface contribute at small $J \ll K, t$, we can project the Hamiltonian onto the band with a Fermi surface, with a dispersion for the band and the spin liquid fermions being equal to $-t\epsilon(k)$ and $K\epsilon(k)$ respectively. The calculations then can be done analytically; we will restrict ourselves to the simplest case $\mu = 0$. Summing the leading logarithmic ladder diagrams, we find the critical temperature T_{c2} is defined by the condition $J\chi_{1e}(T_{c2}) = 1$, where

$$\chi_{1e}(T) = \frac{1}{2} \int \frac{d^3k}{(2\pi)^3} \frac{\tanh\left[\frac{\beta t \epsilon(\mathbf{k})}{2}\right] + \tanh\left[\frac{\beta K \epsilon(\mathbf{k})}{2}\right]}{2(K+t)\epsilon(\mathbf{k})}, \quad (12)$$

is the charge e pairing susceptibility[24]. To logarithmic accuracy, $\chi_{1e}(T) = \frac{\rho}{1+K/t} \ln[W/T]$, where $\rho = 2\sqrt{3}/\pi^2 t$ is the conduction density of states, giving $T_{c2} = W \exp\left(-\frac{1+K/t}{\rho J}\right)$, so a phase transition into the order fractionalized state will occur for *arbitrarily small* Kondo coupling. Of course, deviations from particle-hole symmetry at finite chemical potential destroy the nesting, so when $\mu \neq 0$, a transition takes place at finite $J > J_C$ from an FL* state[25] with a small Fermi surface, into the order-fractionalized state (Fig. 3a). The important point however, is that in the vicinity of particle-hole symmetry, the broken symmetry state is rigorously established.

Below T_{c2} the vector Majorana modes are gapped, leaving behind a single, coherent Majorana mode $c_{\mathbf{k}}^0$ of the conduction electrons. This feature is robust and is related to the mismatch between the quantum numbers of the itinerant Dirac fermions and Majorana triplet of the Yao-Lee spin liquid. The spectrum of the gapped fermions close to the Fermi surface is given by

$$E_{\pm} = (K-t)\epsilon(\mathbf{k})/2 \pm \sqrt{(K+t)^2\epsilon^2(\mathbf{k})/4 + |V|^2}. \quad (13)$$

To understand the nature of the fractionalized order, it is useful to consider the fractionalized order parameter $\hat{v}(\mathbf{x}_j) =$

$-J(\vec{\sigma} \cdot \vec{\chi}_j)c_j$. This quantity carries a Z_2 charge, and by Elitzur's theorem, can not develop long range order. On the other hand, we know that the χ_j field represents a physical degree of freedom at low temperatures, where Z_2 fluctuations have become massive. To reconcile this situation, we must consider the gauge invariant density matrix

$$\rho(x, y) = \langle \hat{v}(\mathbf{x})W(\mathbf{x}, \mathbf{y})\hat{v}^\dagger(\mathbf{y}) \rangle \xrightarrow{|\mathbf{x}-\mathbf{y}| \rightarrow \infty} V(\mathbf{x})V^\dagger(\mathbf{y}) \quad (14)$$

where $W(\mathbf{x}, \mathbf{y}) = \prod u_{(l+1, l)}$ is a Wilson line connecting the sites \mathbf{x}, \mathbf{y} . Once $T < T_{c1}$ the Wilson lines are not only constants of motion, but they are independent of the path between the two sites \mathbf{x} and \mathbf{y} . We can calculate the gauge invariant quantity in the gauge where $u_{(i, j)} = 1$ so that $W = +1$, and in this way, we can be sure that the gauge invariant density matrix asymptotically factorizes into a product of well-defined spinor order[20]. In short, once $T < T_{c1}$ where the absence of visons guarantees that typical Wilson lines are equal to $+1$, this fractionalized long-range order is guaranteed to develop.

One of the physical manifestations of this fractionalized ODLRO, is the development of long-range tunneling of the electrons through the spin liquid, which manifests through the development of odd-frequency triplet pairing and the emergence of a Majorana Fermi surface (Fig 3b). The self-energy for the electrons that describes the coherent tunneling through the spin liquid is given by

$$\begin{aligned} \Sigma(\mathbf{k}, \omega) &= (1 - \mathcal{Z}\mathcal{Z}^\dagger)\Sigma_0(\mathbf{k}, \omega), \\ \Sigma_0(\mathbf{k}, \omega) &= \frac{V^2}{\omega - Kh(\mathbf{k})}. \end{aligned} \quad (15)$$

Here $\mathcal{Z} = \frac{1}{\sqrt{2}}(z_\uparrow, z_\downarrow, -z_\downarrow^*, z_\uparrow^*)^T$ is a Ballian Werthammer spinor, and the combination $P = \mathcal{Z}\mathcal{Z}^\dagger$ projects out the unhybridized scalar component of the conduction sea. Without

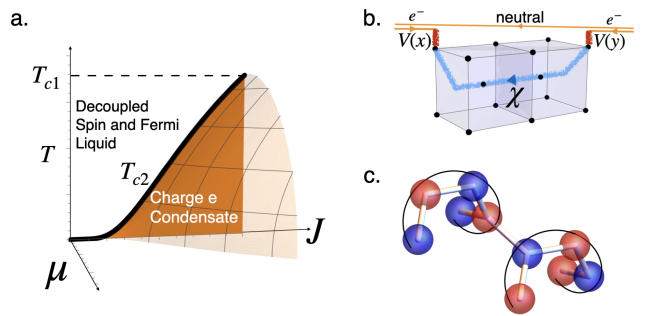


FIG. 3. a) Schematic Phase diagram for the 3D CPT model: below T_{c1} , the Majorana fermions in the spin liquid become phase coherent and at T_{c2} the charge e condensate develops. At particle-hole symmetry ($\mu = 0$) the charge e condensate forms for arbitrarily small Kondo coupling. b) Development of coherent charge e condensate allows tunneling through the spin liquid over arbitrarily long distances, liberating a coherent, quasi-neutral conduction mode. c) Staggered configuration of the gap function $\Delta(R) \sim e^{i2\mathbf{Q}\cdot\mathbf{R}}(\hat{\mathbf{d}}^1 + i\hat{\mathbf{d}}^2) \cdot \vec{\sigma}(1, -1, 1, -1)$ at the four sites of the unit cell, forming a pair-density wave.

the projector, this scattering would describe the resonant scattering of electrons in a Kondo insulator, but the elimination of the scalar component means that a tunneling electron that re-emerges into the spin liquid loses all knowledge of its original charge, allowing it to emerge as a hole, producing resonant Andreev scattering. On the Fermi surface, where $h(\mathbf{k})$ has vanishing eigenvalues $\Sigma(\mathbf{k}, \omega) \sim 1/\omega$ describes odd frequency pairing that is infinitely retarded in time. One of the clearest manifestations of long-range order in the charge e order, is that the projective nature of the scattering self-energy remains coherent in momentum space, allowing the residual scalar Majorana conduction electron c_0 to propagate coherently over arbitrarily long distances.

To examine this resonant pairing in more detail, it is useful to construct the composite order parameter, formed from bilinears of the z field,

$$\hat{\mathbf{d}}_j^1 + i\hat{\mathbf{d}}_j^2 = z_j^T (-i\sigma_2)\sigma z_j, \quad \hat{\mathbf{d}}_j^3 = z_j^\dagger \sigma z_j. \quad (16)$$

The triad $(\hat{\mathbf{d}}_j^1, \hat{\mathbf{d}}_j^2, \hat{\mathbf{d}}_j^3)$ describes co-existing magnetic and superconducting order. We can then divide the self-energy into normal and pairing components

$$\Sigma = \Sigma_N + \Delta(\mathbf{k}, \omega)\tau_+ + \Delta^\dagger(\mathbf{k}, \omega)\tau_-, \quad (17)$$

where

$$\begin{aligned} \Sigma_N(\mathbf{k}, \omega) &= \frac{1}{4} \left(3 - (\hat{\mathbf{d}}^3 \cdot \boldsymbol{\sigma}) \tau_3 \right) \Sigma_0(\mathbf{k}, \omega), \\ \Delta(\mathbf{k}, \omega) &= -\frac{1}{4} \left((\hat{\mathbf{d}}^1 + i\hat{\mathbf{d}}^2) \cdot \boldsymbol{\sigma} \right) \Sigma_0(\mathbf{k}, \omega). \end{aligned} \quad (18)$$

Σ_N describes a kind of odd-frequency magnetism (with no onsite magnetic polarization). The second-term $\Delta(\mathbf{k}, \omega)$ in (18) describes a triplet gap function, with a complex d-vector $\hat{\mathbf{d}}^1 + i\hat{\mathbf{d}}^2$ which breaks time-reversal symmetry.

However, hidden from immediate view, is the fact that the Andreev scattering $\Delta(\mathbf{k}, \omega)$ actually describes a pair density wave. To see this, let us now transform our solution back to the original electron gauge. Reversing the transformation (6), we see that in the original gauge $(V_1, V_2, V_3, V_4)_{\mathbf{R}_j} = \exp[i\mathbf{Q} \cdot \mathbf{R}_j](1, -i, 1, i)V_0$. Now the hyper-octagon lattice can be viewed as made of four-atom coils marked by 1, 2, 3, 4 on Fig. 1, arranged on BCC lattice. From (6) it follows that the $\hat{\mathbf{d}}_{1,2}$ alternate along the coil and between the center and corners of the BCC lattice. In other words, the magnetic vector $\hat{\mathbf{d}}^3$ is uniform, but the superconducting d-vector $\hat{\mathbf{d}}_j^1 + i\hat{\mathbf{d}}_j^2$ is staggered between neighboring sites, forming a pair density wave (PDW).

The Goldstone modes and topology. We briefly touch on the topic of collective excitations and topology. As pointed out above, the gauge invariant quantities must connect two V fields at different points by a string of gauge fields. However, below the melting temperature T_{c1} we can safely forget about Z_2 gauge fields and work in a fixed gauge $u_{(i,j)} = 1$. In this situation, the spinor V acquires the status of a true order parameter. Symmetry dictates that well below the transition where the amplitude fluctuations are weak the Ginzburg-Landau free

energy density f for the low energy sector is given by

$$f[x] = \frac{\rho}{2} \left| \left(-i\vec{\nabla} + e\vec{A} \right) z_\sigma \right|^2 + \frac{\vec{B}^2}{8\pi} - g\mu_B \vec{B} \cdot (z^\dagger \vec{\sigma} z) \quad (19)$$

where $\vec{B} = \nabla \times \vec{A}$ and as before, $V_{j\sigma} = (V/\sqrt{2})z_\sigma$. We have also included a Zeeman coupling.

Since the spinor z is defined by three Euler angles, transforming under the double-group $SU(2)$, small fluctuations of the order parameter consist of three Goldstone modes, one of them being higgsed if the condensate is charged. The free energy (19) has been discussed in various contexts, in particular in connection with multi-band superconductivity when the superconducting pairing takes place on Fermi surface consisting of multiple sheets [26, 27]. The case of zero electric charge $e = 0$ emerges in connection with frustrated magnetism [28, 29]. It is distinct from the conventional superconductivity due to the different topology of the order parameter manifold; here it is of the S^3 sphere. Since $\pi_1(SU(2)) = 0$, it forms a fragile superconductor with a Meissner effect, but zero critical current. The existence of the integer-valued topological invariant in three dimensions $\pi_3(SU(2)) = \mathcal{Z}$

$$Q = \frac{i}{24\pi^2} \int d^3x \epsilon_{\mu\nu\lambda} \text{Tr} \left(U^+ \partial_\mu U U^+ \partial_\nu U U^+ \partial_\lambda U \right), \quad (20)$$

where

$$U = \begin{pmatrix} z_\uparrow & -z_\downarrow^* \\ z_\downarrow & z_\uparrow^* \end{pmatrix}. \quad (21)$$

is an $SU(2)$ matrix, suggests a possibility of nontrivial topological defects of the kind found in the Skyrme model of nuclear matter (for a review, see, for example, [30]). The latter model, however, contains a term with four derivatives whose presence is required to prevent the Skyrmions from collapse. It has been argued by [26] and later by [27, 28] that such terms are generated once one takes into account the fluctuating magnetic field. These authors suggested that in this case, the the Ginzburg Landau free energy (19) admits additional knotted solitons, or Hopfion topological configurations [26–28]. However, numerical calculations performed in [31] indicate that the Hopfions are unstable leaving their existence an open question.

Conclusions. We have presented a model of a three dimensional Kondo lattice which exhibits a remarkable range of properties associated with strong correlations. Some of these properties, such as pair density wave formation, have been observed experimentally, others, like odd-frequency pairing and the formation of a neutral Fermi surface, have been a matter of ongoing debate. The success of our approach is based on the fact that we are able to treat the strong correlations exactly in the asymptotic region of weak Kondo coupling.

There are three key aspects to our work. First, the condensate represents a new class of superconductivity, with the fractionalized order parameter that transforms under a double group. This feature leads to a number of robust consequences. In particular, the group topology determines the fragility of

the superconducting order: although it displays diamagnetism (Meissner effect), the critical current is zero. Since the first homotopy $\pi_1(SU(2)) = 0$, there are no vortices, but a nontrivial third homotopy $\pi_3(SU(2)) = \mathbb{Z}$ suggests a possibility of such topological excitations as Hopfions or hedgehogs. The gauge invariant order parameter also breaks time reversal symmetry in a fashion that is protected by Kramers theorem and independent of crystal lattice, thus the transition into this state will not split under strain. Secondly, the proposed superconducting order forms a PDW that coexists with a novel form of magnetic order. This property is related to the fact that the nested Fermi surfaces of the conduction electrons and the Majoranas are centered at different points in the Brillouin zone, so that when an electron enters the spin liquid, it needs to borrow momentum from the condensate. Thirdly, the low temperature excitations are described by a quasi-neutral Fermi surface whose existence is guaranteed by the mismatch between the quantum numbers of electrons and the Majorana spin excitations, and the long-range coherence of the charge e condensate. This guarantees that even in the situation of perfect nesting (half filled conduction band) there is a residual Majorana Fermi surface.

We end by noting that one of the key features of the current model is the stabilization of an underlying Z_2 spin liquid inside a Kondo lattice, by orbital degrees of freedom which decouple by forming a kind of valence bond solid. This is a situation that conceivably, could occur in quantum materials, such as the topological Kondo insulator SmB_6 , which under field, exhibits Quantum oscillations reminiscent of a bulk Fermi surface[32, 33]. This material is thought to involve a quartet spin-state interacting with a conduction sea[34, 35]. It is interesting to speculate that these orbital degrees of freedom may, under some circumstances, freeze into a valence bond-solid, stabilizing an underlying Majorana spin liquid within the Kondo insulator.

Acknowledgments: This work was supported by Office of Basic Energy Sciences, Material Sciences and Engineering Division, U.S. Department of Energy (DOE) under Contracts No. DE-SC0012704 (AMT) and DE-FG02-99ER45790 (PC and AP). PC is grateful for discussions with Premi Chandra, Tom Banks, Yashar Komijani, Eduardo Fradkin and Subir Sachdev and the support of the Aspen Center for Physics under NSF Grant PHY-1607611, where part of this work was completed. AMT is grateful to E. Babaev, M. Shifman and D. Schubring for valuable discussions.

[1] S. Wirth and F. Steglich, *Nature Reviews, Materials* **1**, 16051 (2016).
 [2] A. Ramires and J. L. Lado, *Phys. Rev. Lett.* **127**, 026401 (2021).
 [3] A. Kumar, N. Chao Hu, A. H. MacDonald, and A. C. Potter,

arXiv e-prints (2021), [arXiv:2110.11962](https://arxiv.org/abs/2110.11962).
 [4] Z.-D. Song and B. A. Bernevig, arXiv e-prints (2021), [arXiv:2111.05865](https://arxiv.org/abs/2111.05865).
 [5] N. Read and D. M. Newns, *Journal of Physics C: Solid State Physics* **16**, 3273 (1983).
 [6] P. Coleman, *Phys. Rev. B* **28**, 5255 (1983).
 [7] A. Auerbach and K. Levin, *Physical Review Letters* **57**, 877 (1986).
 [8] A. J. Millis and P. A. Lee, *Phys. Rev. B* **35**, 3394 (1987).
 [9] P. Coleman, *Phys. Rev. Lett.* **59**, 1026 (1987).
 [10] Q. Si, S. Rabello, K. Ingersent, and J. L. Smith, *Nature* **413**, 804 (2001).
 [11] M. Hermanns and S. Trebst, *Phys. Rev. B* **89**, 235102 (2014).
 [12] M. Hermanns, S. Trebst, and A. Rosch, *Phys. Rev. Lett.* **115**, 177205 (2015).
 [13] U. F. P. Seifert, T. Meng, and M. Vojta, *Physical Review B* **97**, 085118 (2018).
 [14] W. Choi, P. W. Klein, A. Rosch, and Y. B. Kim, *Phys. Rev. B* **98**, 155123 (2018).
 [15] V. S. de Carvalho, R. M. P. Teixeira, H. Freire, and E. Miranda, *Phys. Rev. B* **103**, 174512 (2021).
 [16] C. S. de Farias, V. S. de Carvalho, E. Miranda, and R. G. Pereira, *Phys. Rev. B* **102**, 075110 (2020).
 [17] H. Yao and D.-H. Lee, *Phys. Rev. Lett.* **107**, 087205 (2011).
 [18] A. Kitaev, *Annals of Physics* **321**, 2 (2006).
 [19] Y. Komijani, A. Toth, P. Chandra, and P. Coleman, “Order fractionalization,” (2018), [arXiv:1811.11115](https://arxiv.org/abs/1811.11115).
 [20] A. M. Tsvelik and P. Coleman, “Order Fractionalization in a Kitaev-Kondo model,” (2021), [arXiv:2112.07781](https://arxiv.org/abs/2112.07781).
 [21] U. F. P. Seifert, X.-Y. Dong, S. Chulliparambil, M. Vojta, H.-H. Tu, and L. Janssen, *Phys. Rev. Lett.* **125**, 257202 (2020).
 [22] P. A. Mishchenko, Y. Kato, and Y. Motome, *Phys. Rev. B* **96**, 125124 (2017).
 [23] T. Eschmann, P. A. Mishchenko, K. O’Brien, T. A. Bojesen, Y. Kato, M. Hermanns, Y. Motome, and S. Trebst, *Physical Review B* **102**, 075125 (2020).
 [24] See Supplementary Material.
 [25] T. Senthil, S. Sachdev, and M. Vojta, *Phys. Rev. Lett.* **90**, 216403 (2003).
 [26] E. Babaev, L. D. Faddeev, and A. J. Niemi, *Phys. Rev. B* **65**, 100512 (2002).
 [27] E. Babaev, *Phys. Rev. B* **79**, 104506 (2009).
 [28] C. Naya, D. Schubring, M. Shifman, and Z. Wang, “Skyrmions and hopfions in 3d frustrated magnets,” (2021), [arXiv:2111.06385](https://arxiv.org/abs/2111.06385) [cond-mat.str-el].
 [29] C. D. Batista, M. Shifman, Z. Wang, and S.-S. Zhang, *Phys. Rev. Lett.* **121**, 227201 (2018).
 [30] G. Holzwarth and B. Schwesinger, *Reports on Progress in Physics* **49**, 825 (1986).
 [31] J. Jäykkä, J. Hietarinta, and P. Salo, *Phys. Rev. B* **77**, 094509 (2008).
 [32] B. S. Tan, Y.-T. Hsu, B. Zeng, M. C. Hatnean, N. Harrison, Z. Zhu, M. Hartstein, M. Kiourlappou, A. Srivastava, M. D. Johannes, T. P. Murphy, J.-H. Park, L. Balicas, G. G. Lonzarich, G. Balakrishnan, and S. E. Sebastian, *Science* **349**, 287 (2015).
 [33] O. Erten, P.-Y. Chang, P. Coleman, and A. M. Tsvelik, *Phys. Rev. Lett.* **119**, 057603 (2017).
 [34] V. Alexandrov, M. Dzero, and P. Coleman, *Phys. Rev. Lett.* **111**, 226403 (2013).
 [35] M. Legner, A. Rüegg, and M. Sgrist, *Phys. Rev. Lett.* **115**, 156405 (2015).

Supplemental Material for “A solvable 3D Kondo lattice exhibiting pair density wave, odd-frequency pairing and order fractionalization”

Piers Coleman,^{1,2} Aaditya Panigrahi,¹ and Alexei Tsvelik³

¹*Center for Materials Theory, Department of Physics and Astronomy, Rutgers University, 136 Frelinghuysen Rd., Piscataway, NJ 08854-8019, USA*

²*Department of Physics, Royal Holloway, University of London, Egham, Surrey TW20 0EX, UK.*

³*Division of Condensed Matter Physics and Materials Science, Brookhaven National Laboratory, Upton, NY 11973-5000, USA*

(Dated: July 21, 2022)

1. T_c and the logarithmic divergence in the pair susceptibility

The nesting of the Fermi surfaces between the band electrons and the Majorana fermions generates logarithmic singularities in ladder type diagrams. This nesting originates from the simple fact that the electrons and the Majoranas live on the same lattice and have the identical (up to a factor) tight binding Hamiltonians. We can calculate the transition temperature T_c to logarithmic accuracy by computing the leading logarithmic divergence in the charge e pair susceptibility.

We consider the Hamiltonian

$$H = H_c + H_{YL} + H_K. \quad (1)$$

Below $T_{c1} \sim 0.12K$, the local moments fractionalize $\vec{S}_j \rightarrow -\frac{i}{2}\vec{\chi}_j \times \vec{\chi}_j$, so at half-filling, using equations (3) and (7) of the main text

$$\begin{aligned} H_{YL} &= \frac{K}{2} \sum_{\mathbf{k} \in \text{BZ}} \vec{\chi}_{\mathbf{k}l}^\dagger h(\mathbf{k})_{lm} \vec{\chi}_{\mathbf{k}m}, \\ H_c &= -t \sum_{\mathbf{k} \in \text{BZ}} c_{\mathbf{k}\sigma l}^\dagger h(\mathbf{k})_{lm} c_{\mathbf{k}\sigma m}, \end{aligned} \quad (2)$$

while $h(\mathbf{k})$ is determined by Eq.(4) of the main text,

$$h(\mathbf{k}) = \begin{pmatrix} 0 & i & ie^{-i\mathbf{k}\cdot\mathbf{a}_2} & ie^{-i\mathbf{k}\cdot\mathbf{a}_1} \\ -i & 0 & -i & ie^{-i\mathbf{k}\cdot\mathbf{a}_3} \\ -ie^{i\mathbf{k}\cdot\mathbf{a}_2} & i & 0 & -i \\ -ie^{i\mathbf{k}\cdot\mathbf{a}_1} & -ie^{i\mathbf{k}\cdot\mathbf{a}_3} & i & 0 \end{pmatrix}, \quad (3)$$

The indices $l, m = 1, \dots, 4$ mark different sites in unit cell. The Kondo interaction, taken from equation (1) of the main text is

$$\begin{aligned} H_K &= J \sum_j \left(-\frac{i}{2}\vec{\chi}_j \times \vec{\chi}_j\right) \cdot (c_j^\dagger \vec{\sigma} c_j) \\ &= -\frac{J}{4} \sum_j c_{j\alpha}^\dagger [\sigma^a, \sigma^b]_{\alpha\beta} c_{j\beta} \chi_j^a \chi_j^b, \end{aligned} \quad (4)$$

where we have substituted $\vec{S}_j = -\frac{i}{2}\vec{\chi}_j \times \vec{\chi}_j$ and used the identity $[\sigma^a, \sigma^b] = 2i\epsilon_{abc}\sigma^c$.

We now consider the self-consistent evaluation of the order parameter

$$V_\alpha(l) = \langle (\vec{\sigma}_{\alpha\beta} \cdot \vec{\chi}_l) c_{l\beta} \rangle \quad (5)$$

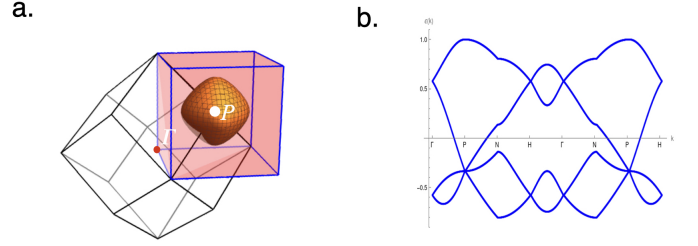


FIG. 1. The Brillouin zone and the dispersion determined by Eq. 5 of the main text.

to leading logarithmic accuracy in perturbation theory, using a Feynman diagram expansion in J . We develop the Feynman diagram expansion in the standard way, starting with a Wick expansion of $Z/Z_0 = \langle T \exp[-\int_0^\beta H_K(\tau) d\tau] \rangle$, to obtain a diagrammatic expansion for the Free energy in terms of linked cluster Feynman diagrams. In the diagrammatic expansion, the bare propagators of conduction electrons and Majorana fermions are diagonal in the spin indices which we omit, and are given by

$$\longrightarrow = G_{lm}^c(k) = [i\omega_n + t\hat{h}(\mathbf{k})]_{lm}^{-1}, \quad (6)$$

for the conduction electrons and

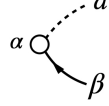
$$\cdots = G_{lm}^M(k) = [i\omega_n - K\hat{h}(\mathbf{k})]_{lm}^{-1}, \quad (7)$$

for Majorana fermions, where the $l, m = 1, 2, 3, 4$ are the site indices and we have also provided the Feynman diagram representation of the propagators. Note the absence of an arrow on the Majorana propagator, which means that when computing Feynman diagrams, one can assign an arrow in either direction to any given Majorana propagator ($G_M(k) = -(G_M(-k))^T$). Diagonalizing the Hamiltonian $\hat{h}(\mathbf{k})_{jl}\psi_\lambda(l, \mathbf{k}) = \epsilon_\lambda(\mathbf{k})\psi_\lambda(j, \mathbf{k})$ we get

$$\begin{aligned} G^c(k)_{lm} &= \sum_{\lambda=0}^3 \frac{\psi_\lambda(l, \mathbf{k})\psi_\lambda^*(m, \mathbf{k})}{i\omega + t\epsilon_\lambda(\mathbf{k})}, \\ G^M(k)_{lm} &= \sum_{\lambda=0}^3 \frac{\psi_\lambda(l, \mathbf{k})\psi_\lambda^*(m, \mathbf{k})}{i\omega - K\epsilon_\lambda(\mathbf{k})} \end{aligned} \quad (8)$$


where $\psi_\lambda(m, \mathbf{k})$ and $\epsilon_\lambda(\mathbf{k})$ are eigenfunctions and eigenvalues of matrix \hat{h} . The resulting spectrum contains four bands; only one band has a Fermi surface (see Fig. 1). Only this one contributes to the logarithmic divergence of the susceptibility. In the following calculation we truncate these Green's functions leaving only the contribution from $\lambda = 0$ mode which crosses the chemical potential.

The Feynman diagram expansion of the Free energy involves the vertices



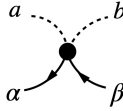
$$= \sigma_{\alpha\beta}^a, \quad (9)$$

and



$$= \langle (\vec{\sigma}_{\alpha\beta} \cdot \vec{\chi}_l) c_{l\beta} \rangle = V_\alpha(l) \quad (10)$$

represents the uniform anomalous order parameter at site l (in the gauge defined by equation (6) of the main text) while the interaction vertex



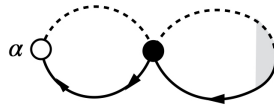
$$= J\Lambda_{\alpha\beta}^{ab} = \frac{J}{2} [\sigma^a, \sigma^b]_{\alpha\beta}, \quad (11)$$

where $\Lambda_{\alpha\beta}^{ab}$ can be written in the convenient form

$$\Lambda_{\alpha\beta}^{ab} = \frac{1}{2} [\sigma^a, \sigma^b]_{\alpha\beta} = [\sigma^a \sigma^b]_{\alpha\beta} - \delta^{ab} \delta_{\alpha\beta}. \quad (12)$$

The reduction of the denominator of (4) from 4 to 2 arises because there are two ways contract the Majorana fermions in the interaction.

To determine the transition temperature we derive a self consistent equation for the pairing amplitude (5), given by



$$= \langle (\vec{\sigma}_{\alpha\beta} \cdot \vec{\chi}_l) c_{l\beta} \rangle = V_\alpha(l) \quad (13)$$

which gives

$$V_\alpha(l) = J \sum_{m=1,4} \chi_{lm}^P V_\alpha(m) \quad (14)$$

where

$$\chi_{lm}^P = -2 \frac{1}{\beta N_s} \sum_{\mathbf{k}, i\omega_n} G_{lm}^C(k) G_{ml}^M(k) \quad (15)$$

Note that the sum over momentum is a sum over the entire Brillouin zone of the BCC lattice. For convenience of calculation, we have used the particle-hole symmetry of the Majorana propagator ($G_{lm}(k) = -G_{lm}(-k)$) to

convert the ‘‘pair’’ susceptibility into a ‘‘particle-hole’’, bubble (hence the -1). The prefactor 2 in the above expression derives from $\Lambda_{\alpha\beta}^{ab} \sigma_\beta^b = 2\sigma_\alpha^a$. (We note that the factor 2 replaces a naive factor of 3 obtained by the Hubbard-Stratonovich transformation, the difference corresponding to the distinction between a Hartree and Hartree-Fock approximation.) We can divide the pair susceptibility into a divergent ‘‘Cooper’’ and a finite interband susceptibility

$$\chi_{lm}^P = \chi_{lm}^C + \chi_{lm}^I \quad (16)$$

The divergent ‘‘Cooper’’ part of this quantity dominates the susceptibility in the limit of low J , and enables us to calculate the transition temperature to leading logarithmic accuracy. This component is obtained by projecting to the $\lambda = 0$ band with a Fermi surface, which gives

$$\begin{aligned} \chi_{lm}^C &= -2 \frac{1}{\beta N_s} \sum_{\mathbf{k}, i\omega_n} \frac{|\psi_0(l, \mathbf{k})|^2 |\psi_0(m, \mathbf{k})|^2}{[i\omega_n + t\epsilon_0(\mathbf{k})][i\omega_n - K\epsilon_0(\mathbf{k})]}, \\ &= -2T \sum_{i\omega_n} \int_{0 < k_l < 2\pi} \frac{d^3 k}{(2\pi)^3} \frac{|\psi_0(l, \mathbf{k})|^2 |\psi_0(m, \mathbf{k})|^2}{[i\omega_n + t\epsilon_0(\mathbf{k})][i\omega_n - K\epsilon_0(\mathbf{k})]}, \end{aligned}$$

Here, we have replaced $\frac{1}{N_s} \sum_{\mathbf{k}} = \frac{1}{2} \int \frac{d^3 k}{(2\pi)^3}$, where the integral is over the Brillouin zone of the BCC lattice (with lattice constant $a = 1$, primitive unit cell volume $a^3/2$ and Brillouin zone volume $(2\pi)^3 / (a^3/2) = 2(2\pi)^3$). We can replace

$$\frac{1}{2} \int_{\mathbf{k} \in BZ} \frac{d^3 k}{(2\pi)^3} = \int_{\mathbf{k} \in 1/2 BZ} \frac{d^3 k}{(2\pi)^3}$$

where the integral is over the half-Brillouin zone defined by $k_l \in [0, 2\pi]$ ($l = 1, 3$).

Now setting $V_\alpha(l) = V_\alpha$, then averaging over sites we can write

$$V_\alpha = J\chi_{1e} V_\alpha \quad (17)$$

where

$$\chi_{1e} = \frac{1}{4} \sum_{m,l=1,4} \chi_{lm}^C. \quad (18)$$

Now since $\sum_{m=1}^4 |\psi_0(m, \mathbf{k})|^2 = 1$, we then obtain

$$\begin{aligned} \chi_{1e} &= -\frac{1}{2} T \sum_n \int \frac{d^3 k}{(2\pi)^3} \frac{1}{[i\omega_n + t\epsilon_0(\mathbf{k})][i\omega_n - K\epsilon_0(\mathbf{k})]} \\ &= \frac{1}{4} \int \frac{d^3 k}{(2\pi)^3} \frac{\text{th}\left(\frac{\beta t\epsilon_0(\mathbf{k})}{2}\right) + \text{th}\left(\frac{\beta K\epsilon_0(\mathbf{k})}{2}\right)}{(t+K)\epsilon_0(\mathbf{k})} \end{aligned} \quad (19)$$

corresponding to equation (12) in the main text. We now replace the momentum integral an energy integral over the density of states writing

$$\chi_{1e} \approx \frac{1}{4} \int_{-W}^W d\epsilon \rho(\epsilon) \frac{\text{th}\left(\frac{\beta\epsilon}{2}\right) + \text{th}\left(\frac{\beta K\epsilon}{2t}\right)}{(1+K/t)\epsilon}, \quad (20)$$

where

$$\rho(E) = \frac{1}{2} \int_{\mathbf{k} \in BZ} \frac{d^3 k}{(2\pi)^3} \delta(E + t\epsilon(\mathbf{k})), \quad (21)$$

where the factor of $1/2$ arises because the volume of the Brillouin zone is $2(2\pi)^3$, and W is the nominal bandwidth. To obtain the logarithmically divergent part of the susceptibility, we can approximate $\rho(E)$ by its value (see section 2. eq (32) below)

$$\rho_e = \rho(0) = \frac{2\sqrt{3}}{\pi^2 t}, \quad (22)$$

which then gives

$$\chi_{1e}(T) = \frac{\rho_e}{(1 + K/t)} \ln\left(\frac{W}{T}\right) \quad (23)$$

Thus, to logarithmic accuracy the critical temperature T_{c2} is determined by

$$1 = J\chi_{1e}(T_{c2}) = \frac{\rho_e J}{1 + K/t} \ln\left(\frac{W}{T_{c2}}\right), \quad (24)$$

The logarithmic divergence means that below

$$T_c = W \exp\left[-\frac{(1 + K/t)}{J\rho_e}\right], \quad (25)$$

corresponding to Eq. (12) of the main text.

2. Calculation of the density of states

Here we calculate the density of states of the conduction electrons and Majorana fermions at the Fermi energy. The energies of the conduction electrons and Majorana fermions in the spin liquid are $-t\epsilon(\mathbf{k}) - \mu$ and $K\epsilon(\mathbf{k})$, where $\epsilon = \epsilon(\mathbf{k})$ is an root of the quartic equation (5) in the main text

$$D(\epsilon) = \epsilon^4 - 6\epsilon^2 - 8\epsilon(s_x s_y s_z) + [4(c_x^2 + c_y^2 + c_z^2) - 3] = 0, \quad (26)$$

where $c_l = \cos(k_l/2)$ and $s_l = \sin(k_l/2)$, ($l = 1, 3$). We shall consider the case where $\mu = 0$. The Fermi surface is determined by the condition that $\epsilon(\mathbf{k}) = 0$, or

$$c_0 = \sqrt{c_x^2 + c_y^2 + c_z^2} = \frac{\sqrt{3}}{2} \quad (27)$$

which describes an approximately spherical Fermi surface centered around $\mathbf{k} = (\pi, \pi, \pi)$ of radius $|k| \sim \pi/(3a)$. We wish to calculate the density of states at the Fermi energy

$$\rho = \frac{1}{2} \int_{\mathbf{k} \in BZ} \frac{d^3 k}{(2\pi)^3} \delta(t\epsilon(\mathbf{k})) = \frac{1}{t} \int_{0 < k_l < 2\pi} \frac{d^3 k}{(2\pi)^3} \delta(\epsilon(\mathbf{k})),$$

where the integral is over the cube of side 2π , ($0 < k_l < 2\pi$), $l = (1, 2, 3)$. Note that the volume of the Brillouin zone for the BCC lattice is $2(2\pi/a)^3$, accounting for the normalization factor of $1/2$ in the momentum integral. We are able to reduce the integral to half the Brillouin zone (the Majorana Brillouin zone) using the fact that $\epsilon(\mathbf{k}) = -\epsilon(-\mathbf{k})$. It is convenient to change variables from momenta $\mathbf{k} = (k_x, k_y, k_z)$ to $\mathbf{c} = (c_x, c_y, c_z)$, because in these co-ordinates, the Fermi surface is a sphere of radius $|\mathbf{c}| = c_0 = \sqrt{3}/2$. Since $dc_l = -\frac{1}{2} \sin(k_l/2) dk_l$ ($l = 1, 3$), it follows that

$$d^3 k = \frac{8}{s_x s_y s_z} d^3 c \quad (28)$$

so that

$$\rho = \frac{1}{t} \int_{|c_l| < 1} \frac{d^3 c}{\pi^3 s_x s_y s_z} \delta(\epsilon(\mathbf{c})) = \frac{1}{t} \int \frac{d\Omega}{\pi^3} \frac{c^2 dc}{s_x s_y s_z} \delta(\epsilon(\mathbf{c})), \quad (29)$$

where we have switch to 3D polar co-ordinates. Now near the Fermi surface we can linearize $D(\epsilon)$

$$D(\epsilon) = -8\epsilon s_x s_y s_z + 4(c^2 - c_0^2) + O(\epsilon^2) \quad (30)$$

so that for small ϵ ,

$$\epsilon = \frac{c^2 - c_0^2}{2s_x s_y s_z}$$

i.e

$$d\epsilon = \frac{cdc}{s_x s_y s_z},$$

so we can simply rewrite (29) as

$$\rho = \frac{c_0}{t} \int \frac{d\Omega}{\pi^3} d\epsilon \delta(\epsilon) = \frac{4\pi c_0}{\pi^3 t} = \frac{2\sqrt{3}}{\pi^2 t}. \quad (31)$$

In a similar fashion, the density of states of the Majorana fermions in the 3D Yao Lee model is given by

$$\rho_M = \frac{1}{2K} \int_{0 < k_l < 2\pi} \frac{d^3 k}{(2\pi)^3} \delta(\epsilon(\mathbf{k})) = \frac{2\sqrt{3}}{\pi^2 K}, \quad (32)$$

where the relative factor of $1/2$ appears because the initial integral is restricted to half the Brillouin zone.

Acknowledgments: This work was supported by the Office of Basic Energy Sciences, Material Sciences and Engineering Division, U.S. Department of Energy (DOE) under Contracts No. DE-SC0012704 (AMT) and DE-FG02-99ER45790 (PC and AP).